Immune Netw. 2021 Aug;21(4):e30
https://doi.org/10.4110/in.2021.21.e30
pISSN 1598-2629·eISSN 2092-6685

IMMUNE NETWORK

Original Article

Check for updates

Mitofusin-2 Promotes the Epithelial-Mesenchymal Transition-Induced Cervical Cancer Progression

Sung Yong Ahn [1,†], **Jiwon Song** [1,2], **Yu Cheon Kim** [1,2], **Myoung Hee Kim** [1,2], **Young-Min Hyun** [1,2,*]

[1]Department of Anatomy, Brain Korea 21 Project, Yonsei University College of Medicine, Seoul, Korea
[2]Graduate School of Medical Science, Brain Korea 21 Project, Yonsei University College of Medicine, Seoul, Korea

OPEN ACCESS

Received: May 11, 2021
Revised: Jul 14, 2021
Accepted: Jul 17, 2021

***Correspondence to**
Young-Min Hyun
Department of Anatomy, Yonsei University College of Medicine, 50-1 Yonsei-ro, Seodaemun-gu, Seoul 03722, Korea.
E-mail: ymhyun@yuhs.ac

[†]Current address: Department of Physiology, Ewha Womans University College of Medicine, Seoul, Korea

ORCID iDs
Sung Yong Ahn
https://orcid.org/0000-0002-6029-1853
Jiwon Song
https://orcid.org/0000-0001-6416-044X
Yu Cheon Kim
https://orcid.org/0000-0002-6123-0729
Myoung Hee Kim
https://orcid.org/0000-0001-5652-1452
Young-Min Hyun
https://orcid.org/0000-0002-0567-2039

Conflict of Interest
The authors declare no potential conflicts of interest.

ABSTRACT

High expression of mitofusin-2 (MFN2), a mitochondrial fusion protein, has been frequently associated with poor prognosis of patients with cervical cancer. Here, we aimed to identify the function of MFN2 in cervical cancer to understand its influence on disease prognosis. To this end, from cervical adenocarcinoma, we performed an MTT assay and quantitative RT-PCR (qRT-PCR) analysis to assess the effects of MFN2 on the proliferation and of HeLa cells. Then, colony-formation ability and tumorigenesis were evaluated using a tumor xenograft mouse model. The migration ability related to MFN2 was also measured using a wound healing assay. Consequently, epithelial-mesenchymal transition (EMT) of MFN2-knockdowned HeLa cells originating from adenocarcinoma. markers related to MFN2 were assessed by qRT-PCR. Clinical data were analyzed using cBioPortal and The Cancer Genome Atlas. We found that MFN2 knockdown reduced the proliferation, colony formation ability, migration, and *in vivo* tumorigenesis of HeLa cells. Primarily, migration of MFN2-knockdowned HeLa cells decreased through the suppression of EMT. Thus, we concluded that MFN2 facilitates cancer progression and *in vivo* tumorigenesis in HeLa cells. These findings suggest that MFN2 could be a novel target to regulate the EMT program and tumorigenic potential in HeLa cells and might serve as a therapeutic target for cervical cancer. Taken together, this study is expected to contribute to the treatment of patients with cervical cancer.

Keywords: MFN2; Oncogene; Epithelial mesenchymal transition

INTRODUCTION

Cervical cancer is the second most common cancer among women worldwide, accounting for approximately 85% of cervical cancer cases in developing countries (1). Cervical cancer is characterized by the unregulated proliferation, migration, and invasion of cervical cells (1). Cervical cancer accounts for 12% of all cancers worldwide and is the most common gynecological malignancy globally (2). High-risk human papillomavirus and various factors, such as sexual or reproductive, environmental or lifestyle-risk, and genetic factors, contribute towards the development of cervical cancer (3). However, the prognosis of cervical cancer is still lacking, and the molecular mechanism underlying its progression is unclear.

IMMUNE NETWORK

Abbreviations

MFN2, mitofusin-2; qRT-PCR, quantitative RT-PCR; EMT, epithelial-mesenchymal transition; TCGA, The Cancer Genome Atlas; OMM, outer mitochondrial membrane; siRNA, small interfering RNA; shRNA, short hairpin RNA; FBS, fetal bovine serum; RPMI, Roswell Park Memorial Institute; CLDN1, Claudin1; OCLN, Occludin; BITC, benzyl isothiocyanate.

Author Contributions

Conceptualization: Hyun YM; Data curation: Song J; Funding acquisition: Hyun YM; Investigation: Ahn SY, Song J, Kim YC; Methodology: Ahn SY; Supervision: Kim MH, Hyun YM; Writing - original draft: Ahn SY, Song J, Hyun YM; Writing - review & editing: Hyun YM.

Mitochondria are essential organelles involved in various metabolic functions, including energy production via oxidative phosphorylation. In cells, mitochondria undergo frequent fission and fusion processes. These play an important role in maintaining mitochondrial function during metabolic or environmental stress (4). The balance between mitochondrial fission and fusion affects mitochondrial morphology and function (5). MFN2, a protein located on the outer mitochondrial membrane (OMM), plays a crucial role in mitochondrial fusion and contributes to the maintenance and activity of mitochondria (6). The OMM GTPase MFN2 was initially identified in the vascular smooth muscle cells of spontaneously hypertensive rats (7). Several mutations in MFN2 are associated with Charcot-Marie-Tooth disease type 2A (8). Moreover, altered MFN2 expression is related to various pathological conditions, including diabetes (9), obesity (10), atherosclerosis (6), Alzheimer's disease (11), Parkinson's disease (8), cardiomyopathy (12), and cancer (10). MFN2 is associated with cancer progression; however, its role in cancer remains unclear. Several studies have indicated that MFN2 is a tumor suppressor; for instance, MFN2 expression is lower in lung (13), colorectal (10), gastric (11), and liver (14) cancer tissues than in normal tissues. In a recent study, MFN2 knockdown in MCF7 and A549 cells elevated the proliferation, colony formation ability, and invasion of cancer cells (15). Additionally, overexpression of MFN2 in urinary bladder carcinoma cell lines inhibited the proliferation of cancer cells by inducing cell cycle arrest and apoptosis (16). However, a recent study showed that MFN2 acts as an oncogene in gastric cancer (17). Furthermore, MFN2 reportedly inhibits the proliferation, migration, and invasion of lung adenocarcinoma cells (18). Therefore, it is necessary to identify the role of MFN2 in cancer pathogenesis.

In a previous study, we showed a positive association between MFN2 expression and cervical cancer pathogenesis through an MFN2 knockdown system using small interfering RNA (siRNA) (19). However, our previous study was unsuitable for long-term experiments because the MFN2 knockdown system using siRNA induced a transient decrease in MFN2 expression. For this reason, in the present study, we performed long-term experiments on a tumor xenograft model generated through the MFN2 knockdown system using short hairpin RNA (shRNA). This study aimed to propose a correlation between MFN2 expression and cervical cancer progression.

MATERIALS AND METHODS

Cell lines and culture

HeLa cell lines originating from adenocarcinoma were cultured in Roswell Park Memorial Institute (RPMI)-1640 medium (Cytiva, Marlborough, MA, USA) containing 10% fetal bovine serum (FBS; Atlas Biologicals, Fort Collins, CO, USA), 100 U/ml penicillin, and 0.1 mg/ml streptomycin-amphotericin B (Lonza, Basel, Switzerland). Puromycin (2 μg/ml; Sigma-Aldrich, St. Louis, MO, USA) was added to the medium to maintain RNA interference in HeLa cells. The cells were incubated at 37°C with 5% CO_2.

Immunocytochemistry

HeLa cells (0.2×10^5 cells/well) were plated onto coverslips in a 12-well plate, fixed with 4% paraformaldehyde, and washed with PBS. The cells were permeabilized with 0.2% Triton X-100 in PBS and blocked with 1% BSA for 1 h at room temperature. Cells were then incubated with the diluted primary Ab, in 1% BSA, against MFN2 (1:200) (Abcam, Cambridge, United Kingdom) at 4°C overnight. Then, the cells were washed thrice with PBS and incubated with

https://doi.org/10.4110/in.2021.21.e30

a secondary Ab (1:1,000), in 1% BSA, for 1 h at room temperature. After washing, the cells on coverslips were mounted using a mounting medium and analyzed under a microscope at the indicated magnifications.

shRNA treatment

For shRNA treatment, HeLa cells were transduced with MFN2-human shRNA lentiviral particles (TL311490VA_ GAGGTTCTTGACTCACTTCAGAGCAAA GC or TL311490VB_ TCAAGTGAGGATGTTTGAGTTTCAGAATT). A scrambled lentiviral shRNA was used as the negative control for MFN2 knockdown (TR30021V; OriGene, Korea).

Proliferation assay

A proliferation assay was performed to investigate whether the expression of MFN2 affects the viability of HeLa cells (20). Proliferation was assessed at three time points: 24, 48, and 72 h. HeLa cells were seeded, at a density of 3×10^3 cells per well, in 96-well plates (SPL, Pocheon, Korea). Then, thiazolyl blue tetrazolium bromide (MTT) solution (Sigma-Aldrich) was diluted with serum-free RPMI-1640 and added to the wells, and the plates were incubated at 37°C and 5% CO_2 for 3 h in the dark. Formazan crystals were solubilized in DMSO (VWR, Radnor, PA, USA). The absorbance was measured at 540 nm using a microplate reader with the SoftMax® Pro software (Molecular Devices, San Jose, CA, USA).

Colony formation assay

A colony formation assay was performed to determine whether MFN2 expression affects the colony-forming ability of HeLa cells (21). HeLa cells were seeded at 800 cells per well in 6-well plates (SPL), and RPMI-1640 medium containing 2 μg/ml puromycin was changed every other day. The plates were incubated at 37°C with 5% CO_2 for 10 days. Formed colonies were fixed with 95% ethanol at 4 °C overnight and stained with 0.25% crystal violet (Sigma-Aldrich), diluted with 20% methanol, at room temperature overnight. The cells were viewed under an inverted research microscope (ECLIPSE Ti2 microscope, Nikon, Tokyo, Japan). The obtained images were quantified using the ImageJ software (18).

Soft agar assay

A soft agar assay was performed to determine whether MFN2 expression affects the anchorage-independent colony-forming ability of HeLa cells. HeLa cells were seeded, at a density of 1×10^4 cells per well, in a 6-well plate (SPL) containing 1 ml of 0.3% low-melting agar in 2× RPMI, supplemented with 20% FBS, and overlaid on a layer containing 1 ml of 1% agar in the same medium. Two weeks later, visible and viable colonies containing >50 cells were counted from five different fields using a stereomicroscope. Representative colonies were photographed. The experiments were performed in triplicate.

Spheroid formation assay

To assess whether MFN2 affects the spheroid-forming ability of HeLa cells, a spheroid formation assay was performed. Briefly, 1×10^4 cells were resuspended in medium using a 25-gauge syringe needle for single-cell suspensions. The cells were pelleted, washed with cold PBS, and filtered again with a syringe to obtain single-cell suspensions. The cells were suspended in 2 ml of DMEM/F12 medium (WelGENE, Gyeongsan, Korea), supplemented with 1% PSA, 2% B27, 20 ng/ml EGF, 10 ng/ml FGFb, 4 μg/ml heparin, and 5 μg/ml insulin, and then seeded in Ultra-Low attachment 6-well plates (Corning, NY, USA). Then, the cells were maintained at 37°C in a 5% CO_2 incubator for 48 h, and the number of spheroids with diameters greater than 100 μm was counted.

https://doi.org/10.4110/in.2021.21.e30

Migration assay

A migration assay was conducted to determine whether MFN2 expression affects the migration ability of HeLa cells (19). Cells in each group were seeded at different densities until 80%–90% confluent because the proliferation rate of MFN2-knockdowned HeLa cells was slower than that of the control cells. HeLa cells were seeded at a density of 2×10^5 cells/well for Scr-shRNA, 3×10^5 cells/well for MFN2-shRNA-1, and 4×10^5 cells/well for MFN2-shRNA-2 in 24-well plates (SPL). When the HeLa cells reached 80%–90% confluency after overnight incubation, the wounds were challenged with 200 μl pipette tips sterilized with an alcohol lamp. Images were captured at 0, 24, and 30 h using the CellSens software (Olympus, Tokyo, Japan).

Western blotting

Western blot analysis was conducted to determine whether MFN2 was knocked down in HeLa cells at the protein level (22). HeLa cell lysates were extracted, and SDS-PAGE was performed to separate proteins by molecular weight. The resolved proteins were transferred onto nitrocellulose membranes (Bio-Rad, Hercules, CA, USA), and after blocking with skimmed milk for 1 h at room temperature, the membranes were incubated at 4°C overnight with an anti-MFN2 Ab (Abcam, Cambridge, United Kingdom) and anti-β-actin Ab (Cell Signaling, Danvers, MA, USA) at a 1:1,000 dilution in 5% blocking solution. Each sample was incubated with the corresponding secondary Abs, and protein bands were visualized using an enhanced chemiluminescence detection system (GW Vitek, Seoul, Korea).

Quantitative RT-PCR (qRT-PCR)

Total RNA was extracted from HeLa cells using TRIzol™ reagent (Invitrogen, Waltham, MA, USA), and cDNA was synthesized using AccuPower RT PreMix (Bioneer, Daejeon, Korea) following the manufacturer's protocol. qRT-PCR was performed using the StepOnePlus system with TB Green Premix Ex Taq II (Takara, Tokyo, Japan). The following primers were used for qRT-PCR: *MFN2*: forward, 5′-GACCTTTGCTCATCTGTGTC-3′ and reverse, 5′-TCCAACCAACCGGCTTTATTC-3′; *β-actin*: forward, 5′-ATAGCACAGCCTGGATAGCAACGTAC-3′ and reverse, 5′-CACCTTCTACAATGAGCTGCGTGTG-3′. The following primers for proliferation markers were used: *PCNA*: forward, 5′-GGCGTGAACCTCACCAGTAT-3′ and reverse, 5′-TTCTCCTGGTTTGGTGCTTC-3′; *Ki67*: forward, 5′-AAGCCCTCCAGCTCCTAGTC-3′ and reverse, 5′-GCAGGTTGCCACTCTTTCTC-3′. The following primers for EMT markers were used: Claudin1 (CLDN1): forward, 5′-GGCTGCTTTGCTGCAACTGTC-3′ and reverse, 5′-GAGCCGTGGCACCTTACACG-3′; Occludin (OCLN): forward, 5′-CGGTCTAGGACGCAGCAGAT-3′ and reverse, 5′-AAGAGGCCTGGATGACATGG-3′; Snail (Snail1): forward, 5′-TCTCTGAGGCCAAGGATCTC-3′ and reverse, 5′-CTTCGGATGTGCATCTTGAG-3′; E-cadherin: forward, 5′-GGTTTTCTACAGCATCACCG-3′ and reverse, 5′-GCTTCCCCATTTGATGACAC-3′; N-cadherin: forward, 5′-TGAAACGGCGGGATAAAGAG-3′ and reverse, 5′-GGCTCCACAGTATCTGGTTG-3′; Axin2: forward: 5′-AAGGGCCAGGTCACCAAAC-3′ and reverse, 5′-CCCCCAACCCATCTTCGT-3′.

Tumor xenograft model

Female BALB/c nude mice (5-wk-old) were purchased from Orient Bio Inc. (Seongnam, Korea). Tumor models were generated via subcutaneous injection of 3×10^6 HeLa cells in the flanks of mice. Tumor volumes were measured using calipers once every 2 days and calculated using the following formula: $V=(L\times W^2)/2$ (L, length; W, width). For puromycin treatment, 10 mg/kg puromycin was subcutaneously injected every 2 days for 18 days. Mice were sacrificed by CO_2 inhalation at the end of the experiment. All mice were maintained

under specific-pathogen-free conditions in the animal establishment at the Avison Biomedical Research Center in Yonsei University College of Medicine.

Bioinformatic analysis

The effect of MFN2 expression in patients with cervical carcinoma was analyzed using cBioPortal and the Human Genome Atlas for cancer genomics. Information on cervical squamous cell carcinoma and endocervical adenocarcinoma was obtained from The Cancer Genome Atlas (TCGA) and Firehose Legacy. In the genomic profiles, mutations and putative copy number alterations from GISTIC were selected. Additionally, mRNA expression z-scores relative to the diploid samples were selected. cBioPortal was used to analyze the mutation count and survival rate of patients with cervical cancer depending on the expression levels of MFN2.

Statistical analysis

Statistical analyses were performed using the IBM SPSS Statistics 26 software. Statistically significant differences among groups were determined with one-way ANOVA followed by Dunnett's *post hoc* test (for proliferation, migration, and colony formation assays). Data are expressed as the mean±SD of values from at least three independent experiments. Statistical significance was determined using two-tailed Student's *t*-tests. Data are expressed as the mean±SEM for tumor volume. Statistical significance was set at $p<0.05$.

Ethics approval and consent to participate

All animal experiments were approved by the Institutional Animal Care and Use Committee of Yonsei University Health System (IACUC 2017-0353).

RESULTS

MFN2 knockdown suppressed the growth of HeLa cells

Using immunohistochemistry, we confirmed that MFN2 was expressed in HeLa cells (**Fig. 1A**). Then, MFN2 was knocked down in HeLa cells via shRNA-mediated transfection. Western blot analysis revealed that MFN2-shRNA transfection inhibited MFN2 expression in HeLa cells compared to that in non-transfected wild-type cells and scrambled shRNA control cells (Scr-shRNA) (**Fig. 1B**).

Compared to that of the Scr-shRNA-transfected HeLa cells, the viability of MFN2-shRNA-transfected cells was significantly decreased at 48–72 h (MFN2-shRNA-1, $p<0.001$) and 24–72 h (MFN2-shRNA-2, $p<0.001$) after transfection (**Fig. 2A**). Furthermore, HeLa cells transfected with MFN2-shRNA showed significantly reduced mRNA levels of Ki67 (both $p<0.001$) and PCNA (both $p<0.001$) relative to those in the Scr-shRNA group (**Fig. 2B**). A colony formation

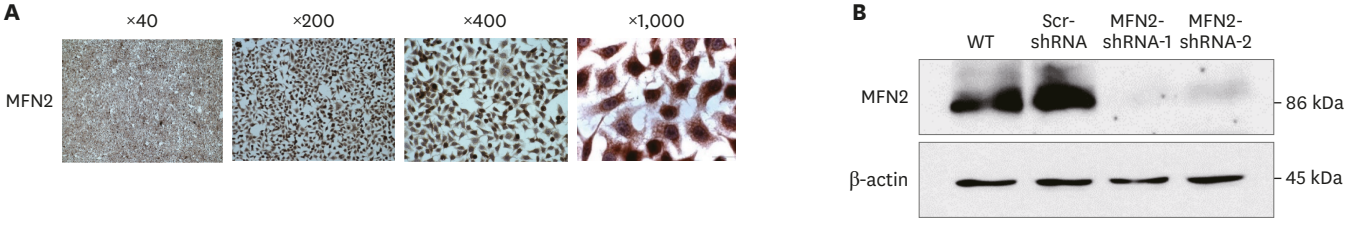

Figure 1. Representative expression of MFN2 in HeLa cells. (A) Immunocytochemistry analysis was conducted to confirm the expression of MFN2 in HeLa cells (original magnification, 40×, 200×, 400×, and 1,000×; scale bar=10 μm). (B) The protein expression of MFN2 was compared between MFN2-shRNA-transfected cells and Scr-shRNA in HeLa cells over time via western blotting. All experiments were performed in triplicate.

https://doi.org/10.4110/in.2021.21.e30

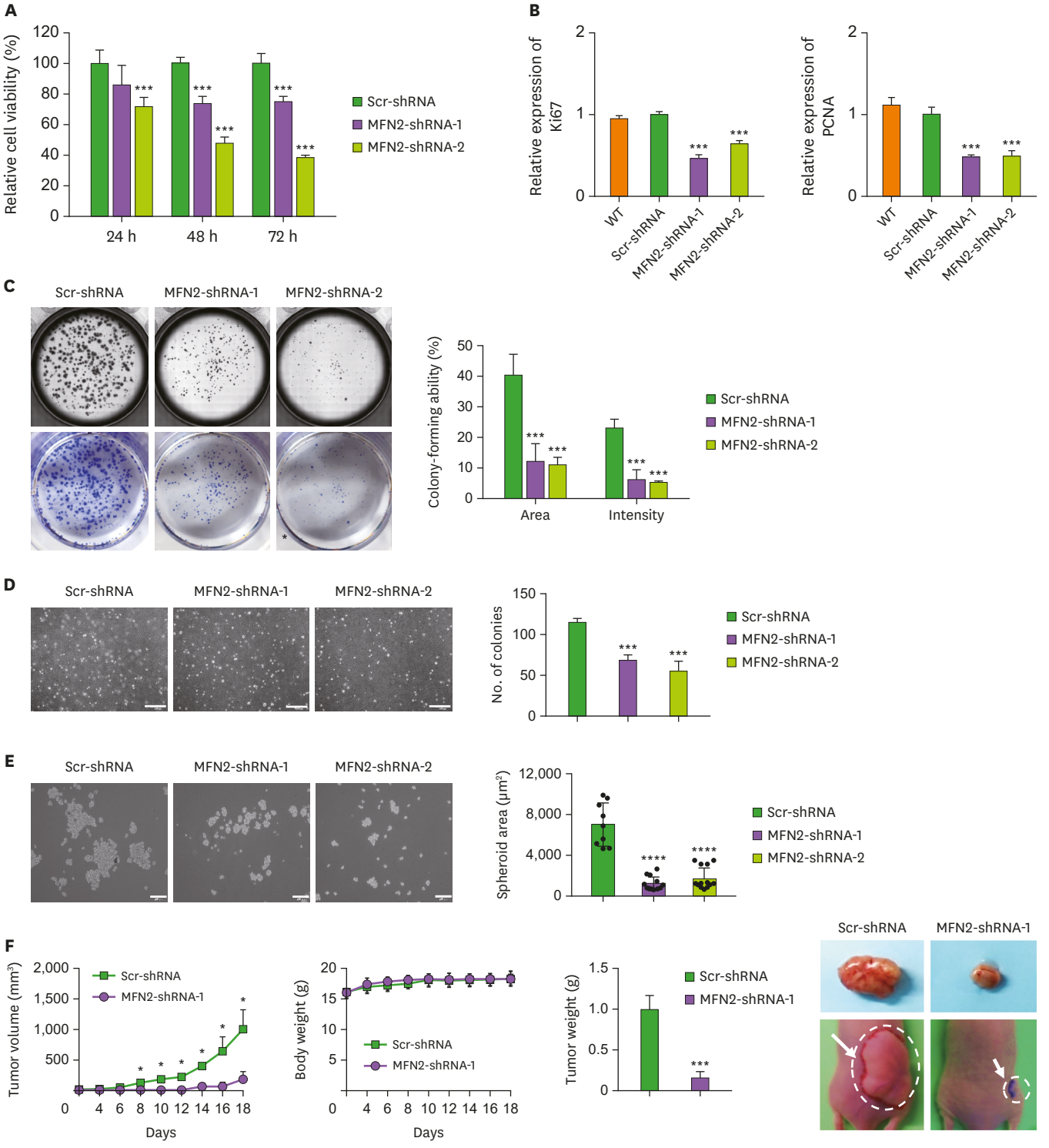

Figure 2. MFN2 knockdown suppressed the growth of HeLa cells. (A) The viability of MFN2-knockdowned cells was significantly reduced compared to that of Scr-shRNA HeLa cells at the indicated time points. (B) The mRNA expression of *Ki-67* and *PCNA* was significantly reduced in MFN2-knockdowned cells compared to that in Scr-shRNA HeLa cells. The results were analyzed using ANOVA followed by Dunnett's *post hoc* test (***p<0.001 vs. Scr-shRNA). (C) Colony-forming ability was significantly reduced in MFN2-knockdowned cells compared to that in the Scr-shRNA HeLa cells. (D) The number of colonies was significantly decreased in MFN2-knockdowned cells compared to that in the Scr-shRNA HeLa cells (original magnification, 40×; scale bar=500 μm). (E) Spheroid formation was significantly inhibited in MFN2-knockdowned cells compared to that in Scr-shRNA HeLa cells at 48 h (original magnification, 100×; scale bar=200 μm). Quantitative spheroid area indicates the mean±SD of values from two independent experiments, each of which was conducted in triplicate (Scr-shRNA; n=9, MFN2-shRNA-1; n=13, MFN2-shRNA-2; n=14). The results were analyzed using one-way ANOVA followed by Dunnett's *post hoc* test (***p<0.001 vs. Scr-shRNA). (F) The tumorigenic ability was significantly attenuated in MFN2-shRNA-1 HeLa cells compared to that in the Scr-shRNA HeLa cells. The results were analyzed using two-tailed Student's *t*-test (*p<0.05 and ***p<0.001 vs. Scr-shRNA) (n=10 mice per group). All experiments were performed in triplicate.

https://doi.org/10.4110/in.2021.21.e30

assay was performed to investigate the effect of MFN2 on HeLa cell colonization. Transfection of MFN2-shRNA remarkably suppressed colony formation in HeLa cells, as measured by colony area (both $p<0.001$) and colony intensity (both $p<0.001$) (**Fig. 2C**). Consistently, compared with that in the corresponding control groups, transfection of MFN2-shRNA significantly decreased the number of colonies of HeLa cells (both $p<0.001$) (**Fig. 2D**). Additionally, the 3-D spheroid formation assay was performed to examine cancer stemness; MFN2 knockdown significantly inhibited the spheroid formation ability of HeLa cells compared to that in the control. These results imply that MFN2 exhibits cancer stem cell-like properties in HeLa cells (**Fig. 2E**). Next, we examined the effect of MFN2 knockdown on tumorigenesis in tumor xenograft models. MFN2 knockdown significantly suppressed *in vivo* tumor growth ($p<0.05$) and relative tumor weight ($p<0.001$) of HeLa cells, whereas the body weight was unaffected (**Fig. 2F**). These results suggest that MFN2 positively regulates tumor growth and progression.

MFN2 knockdown inhibited the migration of HeLa cells

The migratory properties of cancer cells contribute to a poor prognosis in patients. In this study, we investigated the effects of MFN2 on cell migration. The wound-healing assay demonstrated that MFN2 knockdown in HeLa cells significantly suppressed cell migration (**Fig. 3A**). Quantitative analysis of the wound closure rate of HeLa cells revealed that MFN2-shRNA transfection significantly inhibited HeLa cell migration, as measured at 24 h (both $p<0.001$) and 30 h (both $p<0.001$) post scratch wounding (**Fig. 3A**). These findings suggest that MFN2 promotes cancer cell migration.

MFN2 knockdown suppressed Snail-mediated EMT in HeLa cells

EMT is an important biological process implicated in the initiation of metastasis in cancer progression. It is characterized by the loss of the epithelial marker E-cadherin and the gain of the mesenchymal marker N-cadherin (23). We evaluated whether there were differences in the mRNA levels of EMT markers in HeLa cells after MFN2 knockdown. The relative mRNA levels of epithelial markers, Claudin1 (MFN2-shRNA-1, $p<0.05$; MFN2-shRNA-2, $p<0.005$), Occludin (MFN2-shRNA-1, $p<0.05$; MFN2-shRNA-2, $p<0.001$), and E-cadherin (MFN2-shRNA-1, $p<0.001$; MFN2-shRNA-2, $p<0.001$), were significantly increased in MFN2-knockdowned groups compared with those in the scrambled shRNA control (**Fig. 3B**). In contrast, the relative mRNA levels of mesenchymal markers, N-cadherin (MFN2-shRNA-1, $p<0.005$; MFN2-shRNA-2, $p<0.005$) and Axin2 (MFN2-shRNA-1, $p<0.001$; MFN2-shRNA-2, $p<0.001$), were significantly decreased in the MFN2-knockdowned groups (**Fig. 3C**). Additionally, mRNA levels of the EMT-related transcription factor Snail1 (MFN2-shRNA-1, $p<0.001$; MFN2-shRNA-2, $p<0.001$) were significantly decreased after MFN2 knockdown in HeLa cells (**Fig. 3D**). These results suggest that MFN2 acts as a positive regulator of Snail-mediated EMT in HeLa cells.

High MFN2 expression predicted poor prognosis in patients with cervical cancer

To determine the effects of high or low MFN2 expression in patients with cervical cancer, the survival curve for cervical cancer patients with high or low MFN2 mRNA expression was generated from cBioPortal (https://www.cbioportal.org/). We selected human cervical cancer patient samples (n=190) from cervical squamous cell carcinoma and endocervical adenocarcinoma from TCGA. The mutation count was higher in the group with high MFN2 expression than in the group with low MFN2 expression (**Supplementary Fig. 1A**). As shown in **Supplementary Fig. 1B**, cervical cancer patients with high MFN2 expression showed a poor prognosis compared to patients with low MFN2 expression. These results imply that increased levels of MFN2 are associated with poor prognosis in patients with cervical cancer.

https://doi.org/10.4110/in.2021.21.e30

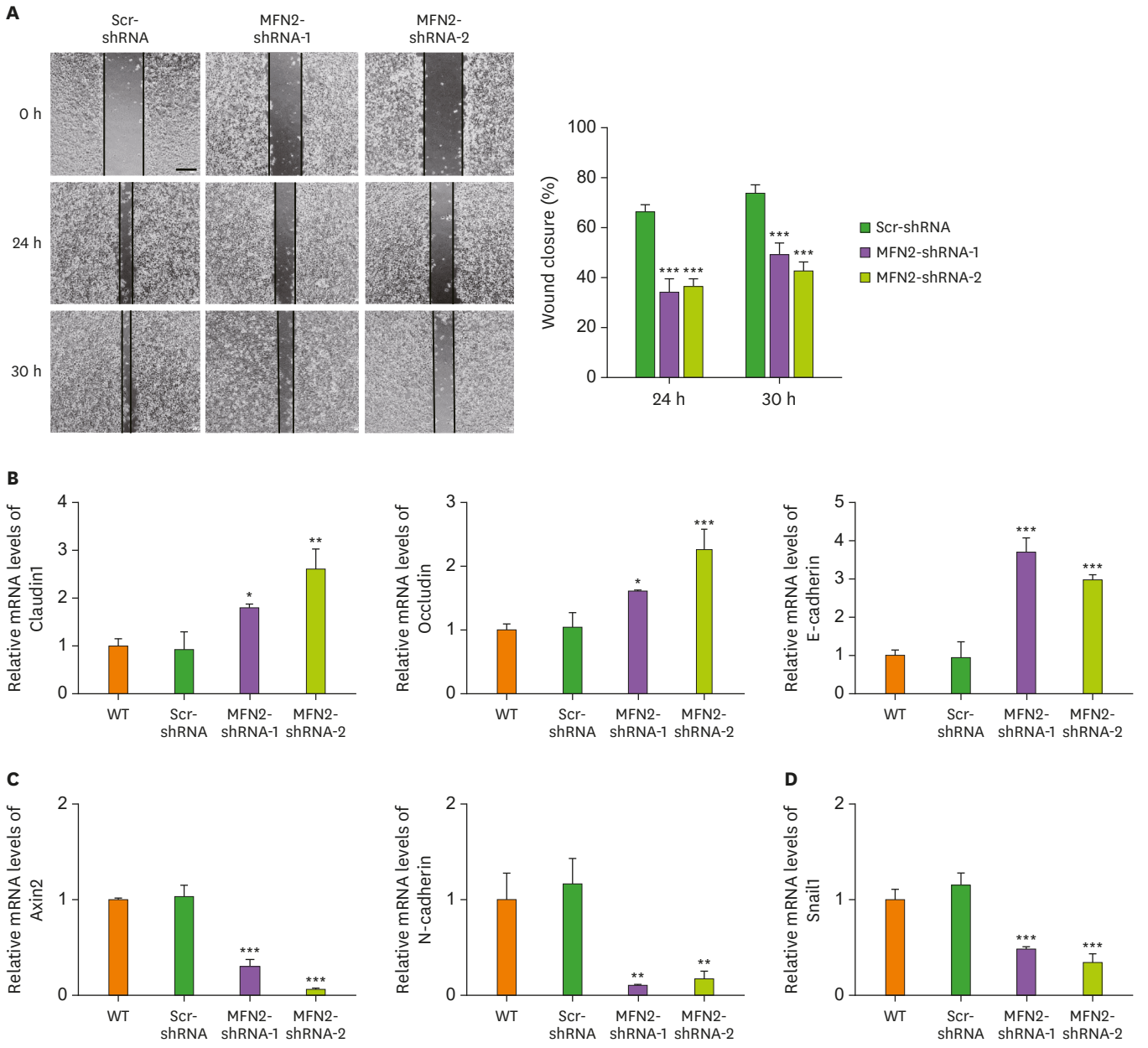

Figure 3. MFN2 knockdown inhibited HeLa cell migration. (A) Cell motility was significantly reduced in MFN2-knockdowned cells compared to that in Scr-shRNA HeLa cells at the indicated time points (original magnification, 100×; scale bar=200 μm). Quantitative results indicate the mean±SD of values from three independent experiments, which were conducted in triplicate (n=9). The results were analyzed with ANOVA followed by Dunnett's *post hoc* test (***p<0.001 vs. Scr-shRNA). (B) The mRNA expression of Claudin1, Occludin, and E-cadherin was significantly increased in MFN2-knockdowned cells compared to that in Scr-shRNA HeLa cells. (C) The mRNA expression of Axin2 and N-cadherin was significantly decreased in MFN2-knockdowned cells compared to that in Scr-shRNA HeLa cells. (D) The mRNA expression of Snail1 was significantly decreased in MFN2-knockdowned cells compared to that in Scr-shRNA HeLa cells. The results were analyzed using one-way ANOVA followed by Dunnett's *post hoc* test (*p<0.05, **p<0.005, ***p<0.001 vs. Scr-shRNA). All experiments were performed in triplicate.

https://doi.org/10.4110/in.2021.21.e30

DISCUSSION

In this study, we investigated whether MFN2 promotes cancer progression in cervical cancer and found that this mitochondrial gene serves as an oncogene in the cervix. The disease prognosis in patients with cervical cancer positively correlated with the expression levels of MFN2. Additionally, the proliferation ability decreased when MFN2 was knocked down in HeLa and SiHa cell lines, which are cervical adenocarcinoma and squamous cell carcinoma cell lines, respectively (24). Most tumors are associated with mitochondrial metabolic dysfunction, which involves excessive fusion and deficient fission under MFN2 overexpression conditions (25,26). Increasing evidence suggests that during cancer progression, cells produce ATP via the mitochondrial oxidative phosphorylation similar to that in normal cells, thus reversing the Warburg effect (27,28). As indicated by Li et al. (27), MFN2 knockdown in non-small cell lung cancer (NSCLC) reduced oxygen consumption, thereby suppressing malignant characteristics such as proliferation, migration, and tumorigenesis (25). Moreover, we discovered that MFN2 promoted Snail-mediated EMT, which leads to the progression of diverse oncogenic functions, including tumor initiation, cancer progression, stemness, migration, metastasis, and resistance to cancer therapy (29,30).

EMT is regulated by various signaling pathways, among which canonical Wnt signaling is a critical pathway that is dependent on the transcription of β-catenin (31,32). In bladder cancer cells, MFN2 inhibits cell proliferation and invasion via the Wnt/β-catenin pathway (33), and in neuronal disease, stress-activated MFN2 regulates the Wnt signaling pathway to exert a neuroprotective function through synapse remodeling (34). Ras signaling is also correlated with MFN2, which regulates cell proliferation, the cell cycle, and morphology by controlling the morphology and tethering of mitochondria and the endoplasmic reticulum (35). In fibroblasts, MFN2 overexpression inhibits cell proliferation and procollagen expression through the Ras-Raf-ERK axis underlying pelvic organ prolapse development (36). Several reports have suggested that modulating MFN2 regulation could be a potential therapeutic strategy against lung injury caused by endotoxins and breast cancer through the PI3K/Akt pathway (37,38). In hypoxic pulmonary hypertension, MFN2 controls pulmonary artery smooth muscle cell proliferation by regulating the PI3K/Akt pathway (39). Moreover, MFN2 regulates the TGF-β pathway, which is the main driver of carcinogenesis (40), and inhibits potential chronic rejection and cellular senescence (41,42). Another report suggested that the dysregulation of Smad, a nuclear-shuttling transcriptional mediator of TGF-β signaling, and MFN2 causes malignant tumor growth and neurodegenerative disorders (43). Finally, MFN2 is indicated as a p53-inducible target gene that suppresses cell proliferation, facilitates apoptosis, and regulates tumor suppression (44).

Benzyl isothiocyanate (BITC), a natural isothiocyanate with antimicrobial activity (45,46), potently inhibits cell motility and matrix metalloproteinase-2 activity in murine melanoma B16F10 cells (46). The inhibition of mitochondrial fusion in breast cancer cell apoptosis by BITC has been reported as an early and important phenomenon. The protein levels of MFN1 and MFN2 were markedly reduced after 2, 4, and 6 h of treatment with BITC in both MDA-MB-231 and MCF-7 breast cancer cells (47). Although BITC reduces the levels of mitochondrial fission-and fusion-related proteins in breast cancer cells, the effect of BITC on cancer-related signaling pathways is unclear. Therefore, future studies on MFN2 and cancer signaling using MFN2 inhibitors are needed.

In conclusion, our study results showed that MFN2 acts as an oncogene that promotes cervical cancer progression, suggesting that *MFN2* could be a new target gene for cervical

cancer treatment. Furthermore, more data related to the incidence of cervical cancer and its association with MFN2 expression might contribute to the identification of novel biomarkers for patients with cervical cancer.

ACKNOWLEDGEMENTS

This research was supported by a grant from the National Research Foundation funded by the Ministry of Science and ICT (MSIT) of the government of Korea (2019R1A2C2008481 to Y.-M.H.).

SUPPLEMENTARY MATERIAL

Supplementary Figure 1

Cervical cancer patients with high MFN2 expression showed a poor prognosis. *In silico* data from patients with cervical cancer correlated with MFN2 expression. (A) Comparison of the mutation count between the groups with high and low MFN2 expression. (B) The overall survival curve for cervical cancer patients with high and low MFN2 expression was acquired from cBioPortal (https://www.cbioportal.org/).

Click here to view

REFERENCES

1. Dasari S, Wudayagiri R, Valluru L. Cervical cancer: biomarkers for diagnosis and treatment. *Clin Chim Acta* 2015;445:7-11.
PUBMED | CROSSREF
2. Senapathy JG, Umadevi P, Kannika PS. The present scenario of cervical cancer control and HPV epidemiology in India: an outline. *Asian Pac J Cancer Prev* 2011;12:1107-1115.
PUBMED
3. Cohen PA, Jhingran A, Oaknin A, Denny L. Cervical cancer. *Lancet* 2019;393:169-182.
PUBMED | CROSSREF
4. Hernández-Alvarez MI, Thabit H, Burns N, Shah S, Brema I, Hatunic M, Finucane F, Liesa M, Chiellini C, Naon D, et al. Subjects with early-onset type 2 diabetes show defective activation of the skeletal muscle PGC-1alpha/Mitofusin-2 regulatory pathway in response to physical activity. *Diabetes Care* 2010;33:645-651.
PUBMED | CROSSREF
5. Bereiter-Hahn J, Vöth M. Dynamics of mitochondria in living cells: shape changes, dislocations, fusion, and fission of mitochondria. *Microsc Res Tech* 1994;27:198-219.
PUBMED | CROSSREF
6. Chien KR, Hoshijima M. Unravelling Ras signals in cardiovascular disease. *Nat Cell Biol* 2004;6:807-808.
PUBMED | CROSSREF
7. Manczak M, Calkins MJ, Reddy PH. Impaired mitochondrial dynamics and abnormal interaction of amyloid beta with mitochondrial protein Drp1 in neurons from patients with Alzheimer's disease: implications for neuronal damage. *Hum Mol Genet* 2011;20:2495-2509.
PUBMED | CROSSREF
8. Lee S, Sterky FH, Mourier A, Terzioglu M, Cullheim S, Olson L, Larsson NG. Mitofusin 2 is necessary for striatal axonal projections of midbrain dopamine neurons. *Hum Mol Genet* 2012;21:4827-4835.
PUBMED | CROSSREF
9. Chen Y, Liu Y, Dorn GW 2nd. Mitochondrial fusion is essential for organelle function and cardiac homeostasis. *Circ Res* 2011;109:1327-1331.
PUBMED | CROSSREF

10. Cheng X, Zhou D, Wei J, Lin J. Cell-cycle arrest at G2/M and proliferation inhibition by adenovirus-expressed mitofusin-2 gene in human colorectal cancer cell lines. *Neoplasma* 2013;60:620-626.
PUBMED | CROSSREF
11. Zhang GE, Jin HL, Lin XK, Chen C, Liu XS, Zhang Q, Yu JR. Anti-tumor effects of Mfn2 in gastric cancer. *Int J Mol Sci* 2013;14:13005-13021.
PUBMED | CROSSREF
12. Xu K, Chen G, Li X, Wu X, Chang Z, Xu J, Zhu Y, Yin P, Liang X, Dong L. MFN2 suppresses cancer progression through inhibition of mTORC2/Akt signaling. *Sci Rep* 2017;7:41718.
PUBMED | CROSSREF
13. Rehman J, Zhang HJ, Toth PT, Zhang Y, Marsboom G, Hong Z, Salgia R, Husain AN, Wietholt C, Archer SL. Inhibition of mitochondrial fission prevents cell cycle progression in lung cancer. *FASEB J* 2012;26:2175-2186.
PUBMED | CROSSREF
14. Wang W, Lu J, Zhu F, Wei J, Jia C, Zhang Y, Zhou L, Xie H, Zheng S. Pro-apoptotic and anti-proliferative effects of mitofusin-2 via Bax signaling in hepatocellular carcinoma cells. *Med Oncol* 2012;29:70-76.
PUBMED | CROSSREF
15. Lin Z, Lin Y, Shen J, Jiang M, Hou Y. Flavonoids in *Ageratum conyzoides* L. Exert potent antitumor effects on human cervical adenocarcinoma HeLa cells *in vitro* and *in vivo*. *BioMed Res Int* 2020;2020:2696350.
PUBMED | CROSSREF
16. Jin B, Fu G, Pan H, Cheng X, Zhou L, Lv J, Chen G, Zheng S. Anti-tumour efficacy of mitofusin-2 in urinary bladder carcinoma. *Med Oncol* 2011;28 Suppl 1:S373-S380.
PUBMED | CROSSREF
17. Fang CL, Sun DP, Chen HK, Lin CC, Hung ST, Uen YH, Lin KY. Overexpression of mitochondrial GTPase MFN2 represents a negative prognostic marker in human gastric cancer and its inhibition exerts anti-cancer effects. *J Cancer* 2017;8:1153-1161.
PUBMED | CROSSREF
18. Guzmán C, Bagga M, Kaur A, Westermarck J, Abankwa D. ColonyArea: an ImageJ plugin to automatically quantify colony formation in clonogenic assays. *PLoS One* 2014;9:e92444.
PUBMED | CROSSREF
19. Cory G. Scratch-wound assay. *Methods Mol Biol* 2011;769:25-30.
PUBMED | CROSSREF
20. Mosmann T. Rapid colorimetric assay for cellular growth and survival: application to proliferation and cytotoxicity assays. *J Immunol Methods* 1983;65:55-63.
PUBMED | CROSSREF
21. Grembecka J, He S, Shi A, Purohit T, Muntean AG, Sorenson RJ, Showalter HD, Murai MJ, Belcher AM, Hartley T, et al. Menin-MLL inhibitors reverse oncogenic activity of MLL fusion proteins in leukemia. *Nat Chem Biol* 2012;8:277-284.
PUBMED | CROSSREF
22. Kurien BT, Scofield RH. Western blotting: an introduction. *Methods Mol Biol* 2015;1312:17-30.
PUBMED | CROSSREF
23. Thiery JP, Acloque H, Huang RY, Nieto MA. Epithelial-mesenchymal transitions in development and disease. *Cell* 2009;139:871-890.
PUBMED | CROSSREF
24. Ahn SY, Li C, Zhang X, Hyun YM. Mitofusin-2 expression is implicated in cervical cancer pathogenesis. *Anticancer Res* 2018;38:3419-3426.
PUBMED | CROSSREF
25. Ghosh P, Vidal C, Dey S, Zhang L. Mitochondria targeting as an effective strategy for cancer therapy. *Int J Mol Sci* 2020;21:21.
PUBMED | CROSSREF
26. Pustylnikov S, Costabile F, Beghi S, Facciabene A. Targeting mitochondria in cancer: current concepts and immunotherapy approaches. *Transl Res* 2018;202:35-51.
PUBMED | CROSSREF
27. Li T, Han J, Jia L, Hu X, Chen L, Wang Y. PKM2 coordinates glycolysis with mitochondrial fusion and oxidative phosphorylation. *Protein Cell* 2019;10:583-594.
PUBMED | CROSSREF
28. Hanahan D, Weinberg RA. Hallmarks of cancer: the next generation. *Cell* 2011;144:646-674.
PUBMED | CROSSREF
29. Pastushenko I, Blanpain C. EMT transition states during tumor progression and metastasis. *Trends Cell Biol* 2019;29:212-226.
PUBMED | CROSSREF

30. Cho ES, Kang HE, Kim NH, Yook JI. Therapeutic implications of cancer epithelial-mesenchymal transition (EMT). *Arch Pharm Res* 2019;42:14-24.
PUBMED | CROSSREF

31. Gajos-Michniewicz A, Czyz M. WNT signaling in melanoma. *Int J Mol Sci* 2020;21:21.
PUBMED | CROSSREF

32. Taciak B, Pruszynska I, Kiraga L, Bialasek M, Krol M. Wnt signaling pathway in development and cancer. *J Physiol Pharmacol* 2018;69:69.
PUBMED

33. Pang G, Xie Q, Yao J. Mitofusin 2 inhibits bladder cancer cell proliferation and invasion via the Wnt/β-catenin pathway. *Oncol Lett* 2019;18:2434-2442.
PUBMED | CROSSREF

34. Palomera-Avalos V, Griñán-Ferré C, Puigoriol-Ilamola D, Camins A, Sanfeliu C, Canudas AM, Pallàs M. Resveratrol protects samp8 brain under metabolic stress: focus on mitochondrial function and wnt pathway. *Mol Neurobiol* 2017;54:1661-1676.
PUBMED | CROSSREF

35. de Brito OM, Scorrano L. Mitofusin-2 regulates mitochondrial and endoplasmic reticulum morphology and tethering: the role of Ras. *Mitochondrion* 2009;9:222-226.
PUBMED | CROSSREF

36. Wang X, Wang X, Zhou Y, Peng C, Chen H, Lu Y. Mitofusin2 regulates the proliferation and function of fibroblasts: the possible mechanisms underlying pelvic organ prolapse development. *Mol Med Rep* 2019;20:2859-2866.
PUBMED | CROSSREF

37. Shi J, Yu J, Zhang Y, Wu L, Dong S, Wu L, Wu L, Du S, Zhang Y, Ma D. PI3K/Akt pathway-mediated HO-1 induction regulates mitochondrial quality control and attenuates endotoxin-induced acute lung injury. *Lab Invest* 2019;99:1795-1809.
PUBMED | CROSSREF

38. Ma LI, Chang Y, Yu L, He W, Liu Y. Pro-apoptotic and anti-proliferative effects of mitofusin-2 via PI3K/Akt signaling in breast cancer cells. *Oncol Lett* 2015;10:3816-3822.
PUBMED | CROSSREF

39. Fang X, Chen X, Zhong G, Chen Q, Hu C. Mitofusin 2 downregulation triggers pulmonary artery smooth muscle cell proliferation and apoptosis imbalance in rats with hypoxic pulmonary hypertension via the PI3K/Akt and mitochondrial apoptosis pathways. *J Cardiovasc Pharmacol* 2016;67:164-174.
PUBMED | CROSSREF

40. Syed V. Tgf-β signaling in cancer. *J Cell Biochem* 2016;117:1279-1287.
PUBMED | CROSSREF

41. Sun Q, Chen L, Zhou D, Yang Q, Song W, Chen D, Wang W. Mfn2 inhibits chronic rejection of the rat abdominal aorta by regulating TGF-β1 levels. *Transpl Immunol* 2019;55:101211.
PUBMED | CROSSREF

42. He H, Yu B, Liu Z, Ye G, You W, Hong Y, Lian Q, Zhang Y, Li X. Vascular progenitor cell senescence in patients with Marfan syndrome. *J Cell Mol Med* 2019;23:4139-4152.
PUBMED | CROSSREF

43. Kumar S, Pan CC, Shah N, Wheeler SE, Hoyt KR, Hempel N, Mythreye K, Lee NY. Activation of mitofusin2 by Smad2-RIN1 complex during mitochondrial fusion. *Mol Cell* 2016;62:520-531.
PUBMED | CROSSREF

44. Wang W, Cheng X, Lu J, Wei J, Fu G, Zhu F, Jia C, Zhou L, Xie H, Zheng S. Mitofusin-2 is a novel direct target of p53. *Biochem Biophys Res Commun* 2010;400:587-592.
PUBMED | CROSSREF

45. Abdel-Kader MS, Kamal YT, Alam P, Alqarni MH, Foudah AI. Quantitative analysis of benzyl isothiocyanate in *Salvadora persica* extract and dental care herbal formulations using reversed phase C18 high-performance liquid chromatography method. *Pharmacogn Mag* 2017;13 Suppl 3:S412-S416.
PUBMED | CROSSREF

46. Lai KC, Hsiao YT, Yang JL, Ma YS, Huang YP, Chiang TA, Chung JG. Benzyl isothiocyanate and phenethyl isothiocyanate inhibit murine melanoma B16F10 cell migration and invasion in vitro. *Int J Oncol* 2017;51:832-840.
PUBMED | CROSSREF

47. Sehrawat A, Croix CS, Baty CJ, Watkins S, Tailor D, Singh RP, Singh SV. Inhibition of mitochondrial fusion is an early and critical event in breast cancer cell apoptosis by dietary chemopreventative benzyl isothiocyanate. *Mitochondrion* 2016;30:67-77.
PUBMED | CROSSREF